HTML ABSTRACT + LINKS

Fluorine segregation and incorporation during solid-phase epitaxy of Si

S. Mirabella,[a] G. Impellizzeri, E. Bruno, L. Romano, M. G. Grimaldi, and F. Priolo
MATIS-INFM and Dipartimento di Fisica e Astronomia, Università di Catania, Via S. Sofia 64, I-95123 Catania, Italy

E. Napolitani and A. Carnera
MATIS-INFM and Dipartimento di Fisica, Università di Padova, Via Marzolo 8, I-35131 Padova, Italy

(Received 5 August 2004; accepted 1 February 2005; published online 14 March 2005)

We report on the F incorporation into Si during solid-phase epitaxy (SPE) at 580 °C and with the presence of B and/or As, clarifying the F incorporation mechanism into Si. A strong segregation of F at the moving amorphous–crystalline interface has been characterized, leading to a SPE rate retardation and to a significant loss of F atoms through the surface. In B- or As-doped samples, an enhanced, local F incorporation is observed, whereas in the case of B and As co-implantation (leading to compensating dopant effect), a much lower F incorporation is achieved at the dopant peak. The F enhanced incorporation with the presence of B or As is shown to be a kinetic effect related to the SPE rate modification by doping, whereas the hypothesis of a F–B or F–As chemical bonding is refused. These results shed new light on the application of F in the fabrication of ultrashallow junctions in future generation devices. © *2005 American Institute of Physics*.
[DOI: 10.1063/1.1886907]

The increasing scaling down of modern ultrashallow junctions for metal–oxide–semiconductor devices represents a strategic challenge for the technological development as well as a charming issue in fundamental research. In particular, the future technological 32 nm node will require dopant activation and confinement in regions shallower than 10 nm.[1] In order to achieve this result, high B fluence implantation in preamorphized Si has been widely studied and the addition of the fluorine ingredient has become more and more interesting, also for the usage of BF_2^+ implantation.[2–8]

Dopant implantation in preamorphized Si has the advantage to avoid both channelling effects and, of course, crystal damaging during the implantation itself. Still, the subsequent recrystallization by solid phase epitaxy (SPE) leaves structural defects beyond the original amorphous–crystalline ($a-c$) interface, commonly referred to as the *end-of-range* defects (EOR).[9] Upon further thermal annealing, needed to electrically activate the dopant, such EOR defects could evolve emitting a backflow of Si self-interstitials (Is) toward the surface. This leads to a dramatic spread of the dopant distribution due to the transient enhanced diffusion (TED).[10]

In such a system the F benefice consists in a strong reduction of boron TED without severely deteriorating the electrical activity of the dopants.[3,4,6,8] As we recently showed, the atomistic mechanism of this F ability cannot be ascribed to a B–F chemical bonding,[6] as suggested instead by Mokhberi *et al.*[4] We concluded that an interaction between F and Is must be assumed to account for the boron TED reduction.[6] Thus, the presence of F in the regrown Si is crucial in order to achieve an ultrashallow B profile. Indeed, an evident redistribution of F after the SPE of preamorphized Si has been observed,[4,6,11,12] even if the evolution of this redistribution, the contributions of F implant conditions or dopant co-implantation, have to be clarified.

The aim of this work is to study the epitaxial regrowth of F implanted Si, characterizing the F segregation phenomenon and its dependence on the presence of B and/or As. The reported results can improve the understanding and the application of F in modern ultrashallow junction fabrication.

Experiments were performed on *n*-type, Si epilayers grown by chemical vapor deposition upon 6 in. (100) Si wafers. Si samples were amorphized from the surface to a depth of ~530 nm by implanting Si^- ions (3×10^{15} ions/cm^2 at 250 keV, plus 2×10^{15} ions/cm^2 at 40 keV) at the liquid nitrogen temperature. The amorphized samples were enriched in fluorine by implanting 100 keV, 4×10^{14} F/cm^2, and some of these were further implanted with B (10 keV, 1×10^{14} or 7.5×10^{14} atoms/cm^2) and/or As (55 keV, 6×10^{14} atoms/cm^2). All the amorphized samples were annealed at 450 °C for 30 min, followed by SPE at 580 °C for 120 min in N_2 atmosphere. The SPE kinetics at 580 °C were characterized in detail by annealing the samples from 15 min up to the complete regrowth (120 min) in a conventional horizontal furnace. By means of Rutherford backscattering spectrometry (RBS) in random and channelling geometry, we measured the residual amorphous thickness after each annealing step as well as the crystalline quality of the regrown layer. Some of the regrown samples were treated by rapid thermal annealing (RTA) in N_2 atmosphere, at 850 °C for 10 min, in order to induce an Is backflow from the EOR region and thus study the F and B diffusion. The concentration depth profiles of B, As, and F were obtained by secondary ion mass spectrometry (SIMS), using a CAMECA IMS-4*f* instrument, by collecting B^+, $(AsSi)^+$, and F^+ secondary ions, respectively, while sputtering with a 3 keV O_2^+ beam.

The epitaxial regrowth kinetics at 580 °C of F implanted Si is shown in Fig. 1(a), where the as-implanted F distribution (dotted line) and the post-SPE one (triangles) are plotted together with the F profile snapshots at four different SPE times [15, 30, 60, and 90 min (continuous lines)]. In addition, the $a-c$ interface positions, as determined by RBS analyses, are reported as vertical lines relative to the partial regrowth experiments. It is clear that, during the SPE process, F atoms accumulate at the $a-c$ interface by which F is

[a]Electronic mail: mirabella@ct.infn.it

 © 2005 American Institute of Physics
Downloaded 08 Jan 2007 to 192.84.150.213. Redistribution subject to AIP license or copyright, see http://apl.aip.org/apl/copyright.jsp

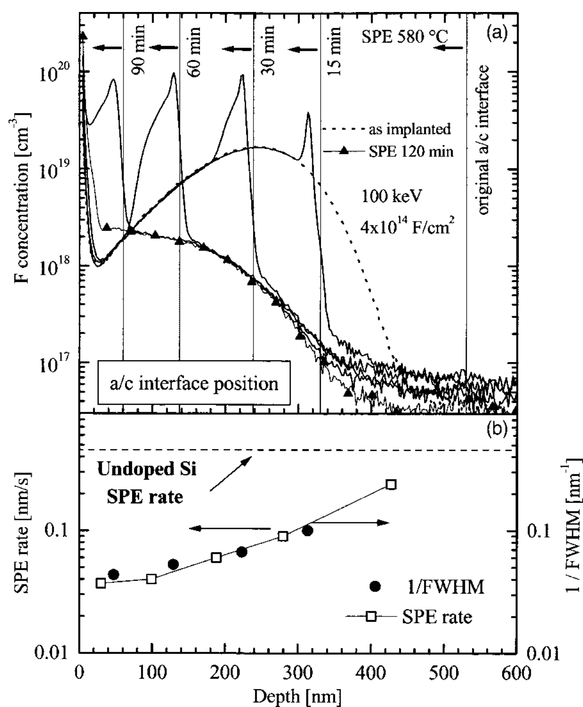

FIG. 1. (a) SIMS profiles of F incorporation after implantation (dotted line, 100 keV, 4×10^{14} at./cm^2), during (continuous lines) and after (triangles) SPE at 580 °C. The a–c interface positions during SPE, as determined by channeling measurements, are also indicated by vertical lines. (b) Averaged SPE rate (squares, left-hand vertical axis) and reciprocal of F peak FWHM (circles, right-hand vertical axis) versus depth. The undoped Si SPE rate at 580 °C (Ref. 13) is reported too (horizontal dashed line).

pushed toward the surface. The F peak is clearly located at the amorphous side of the $a-c$ interface, and, once SPE is completed, this F peak disappears, evaporating from the surface. On the crystalline side, F is incorporated at a concentration about two orders of magnitude lower than the F peak. In fact, the segregation coefficient at the interface, k, defined as the concentration in the crystal over the one in the amorphous at the interface depth, is measured to range from 0.005 to 0.03. This k variability could mean that the system is not in steady-state conditions. As a result of this segregation, we observe that at the end of the SPE only 15% of the F implanted fluence remains in the sample.

From Fig. 1(a) we can also follow the $a-c$ interface motion, whose velocity decreases with time. The average velocity between two consecutive $a-c$ interface positions were calculated and plotted in Fig. 1(b) with open squares (left-hand axis), together with the undoped Si SPE rate (dashed line) at 580 °C.[13] A reduction of the SPE rate up to 10 times with respect to the undoped case is observed, due to the F segregation, in agreement with literature data.[7,12]

In Fig. 1(b), we plotted the reciprocal of the full-width at half-maximum (FWHM) (closed circles, right-hand scale) of the F segregation peaks as extracted from Fig. 1(a). According to the classic segregation theory,[14] the reciprocal of the FWHM of the peak segregated at the $a-c$ interface is equal to the ratio between the SPE rate and the impurity diffusivity in the amorphous phase. In fact, the SPE rate and the impurity diffusivity have opposite effects on the F incorporation, competing the first in favor and the second against it. As shown in Fig. 1(b), the correlation with the SPE rate is quite high, indicating that, in fact, the SPE rate and FWHM are inversely proportional and therefore that F diffusivity in

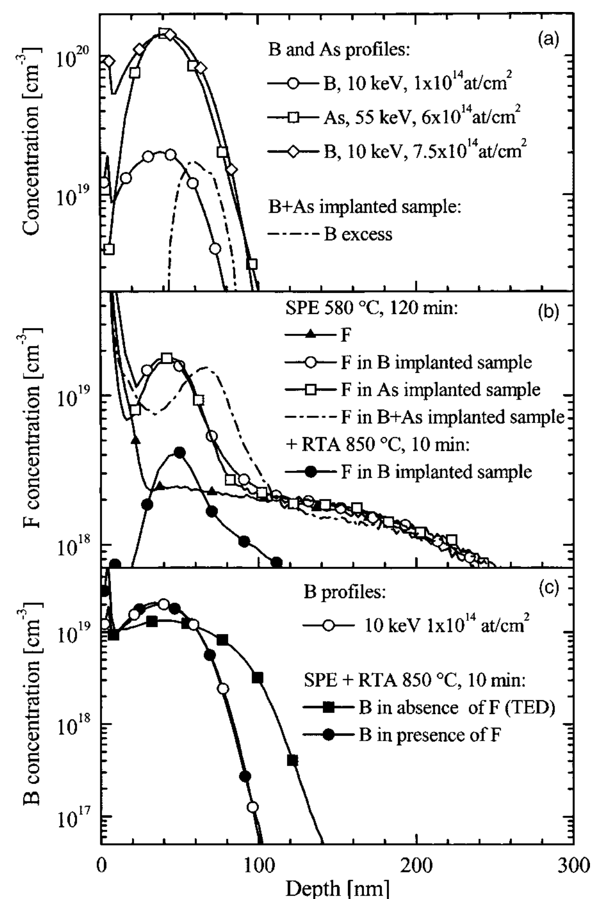

FIG. 2. (a) SIMS profiles of B and As concentration after implantation: 10 keV, 1×10^{14} B/cm^2 (open circles); 55 keV, 6×10^{14} As/cm^2 (open squares); 10 keV, 7.5×10^{14} B/cm^2 (open diamonds, used to compensate the As doped sample). The B atomic excess in the B and As co-implanted sample is shown with a dash-dotted line. (b) SIMS profiles of F concentration after 580 °C SPE in the B- (open circles) or As- (open squares) doped samples, in the B and As co-implanted sample (dash-dotted line), and without any dopant (triangles). F profile in the B doped sample after 850 °C, 10 min RTA is reported too (closed circles). (c) SIMS profiles of B concentration after the SPE and 850 °C, 10 min RTA, in absence (closed squares) or in presence (closed circles) of F. The as-implanted B profile (open circles) is reported as reference.

amorphous Si is constant during the whole regrowth process. Since F diffusivity in amorphous Si will be given by the product between SPE rate and FWHM of the segregation peak, an estimate can be easily done. This gives a value of $(0.9\pm0.1)\times10^{-14}$ cm^2/s at 580 °C, which agrees very well with the F diffusivity in amorphous Si determined by Nash *et al.* with a very different experimental method.[15] This very high diffusivity together with the low segregation coefficient measured explains the substantial F loss we observed after SPE. The time to regrow 1 nm at 580 °C is ~25 s, whereas in the same time F diffusion length in amorphous Si is about 5 nm, hence F can escape the regrowing front.

We also studied the effect of B and/or As on the F incorporation during SPE at 580 °C, taking into account the SPE rate modification by dopants. In Fig. 2(a) the used dopant implant profiles are shown: 10 keV, 1×10^{14} B/cm^2 (open circles); 55 keV, 6×10^{14} As/cm^2 (open squares); and 10 keV, 7.5×10^{14} B/cm^2 (open diamonds). The first two implants were performed separately on different samples, in order to achieve the same SPE rate enhancement by different dopants.[13] The second implant was performed together with the third one on sample to attempt the dopant compensation,

Downloaded 08 Jan 2007 to 192.84.150.213. Redistribution subject to AIP license or copyright, see http://apl.aip.org/apl/copyright.jsp

for which no SPE rate modification occurs.[13]

In Fig. 2(b) the F profiles after the 580 °C SPE are shown in the different samples: B doping (open circles); As doping (open squares); and B and As co-doping (dash-dotted line), together with the case of only F implanted sample (triangles). In the case of B doping, F incorporation [open circles in Fig. 2(b)] is locally enhanced, quantitatively reproducing the B implantation peak. If we now consider the As doping case, the F profile [open squares in Fig. 2(b)] exactly reproduces the previous one, even if the As peak concentration is six times higher than the B one. In both cases, the F incorporation enhancement (F super-incorporation) is of the same factor (almost ten times) with respect to the case of only the F implanted sample [triangles in Fig. 2(b)], regardless of the different dopant amount. It is worth noting that the different dopant dose was used on purpose to obtain the same SPE rate enhancement which, in both cases, doubles the Si undoped SPE rate.[13] Thus, we hypothesize that the F superincorporation is strictly related to the SPE rate, rather than to a direct interaction between F and the dopants.

In order to disclaim this point we did a definitive experiment, by adding B in the As-doped sample in order to attempt the dopant compensation [see open diamonds and squares in Fig. 2(a)]. In fact, if the dopant compensation is achieved no SPE rate enhancement occurs in spite of the dopants co-presence.[13] On the other hand, the dopants copresence would result in a even higher F superincorporation, if the incorporation is due to F chemical bonding with B and/or As. When B and As are co-implanted, the F profile, after the usual SPE, is shown with a dash-dotted line in Fig. 2(b). Actually, we can observe an F peak at a depth ($\sim$60 nm) deeper than the B and As peak depth (40 nm), where, instead, a dip in the F incorporation profile is achieved. This modulation in the F incorporated profile is easily explained in terms of an incomplete compensating dopant effect. As a matter of fact, the B profile equals the As one just at the peak depth, whereas elsewhere, because of a small difference in the implantation straggling, B concentration is slightly higher than As, leading to a *p*-type doped silicon. The difference between B and As is plotted in Fig. 2(a) (dash-dotted line) showing a B maximum excess higher than 1×10^{19} atoms/cm^3 located at the depth of $\sim$60 nm. Note the depth alignment between the F peak and the dopant difference. In addition, the concentration of the F peak comes close to the one in the B-doped sample, as the resulting *p*-type doping is of the same order of magnitude.

The above-mentioned results represent clear evidence that the F superincorporation is not caused by a chemical bonding between F and dopants, whereas it is due to a kinetic effect related to the SPE rate modification. In fact, where the $a-c$ interface has locally moved quicker because of doping,[13] a larger amount of F has no time to diffuse away from the moving interface and is forceably superincorporated in the regrown layer.

Recently, Mokhberi *et al.* reported an F superincorporation in Si just in presence of B, while not in the presence of As.[4] On such a basis, they invoked a B–F chemical bonding, which would be responsible, according to them, also for the boron TED reduction by F. Still, they used a very high dose for the As implant (7 keV, 1×10^{15} atoms/cm^2 resulting in a peak concentration of $\sim 1 \times 10^{21}$ atoms/cm^3)[4] for which the SPE rate is decreased,[13] and then the F incorporation is hindered. On the contrary, for our As concentration peak the SPE rate is enhanced and F is seen to be superincorporated [squares in Fig. 2(b)]. Since our results unambiguously exclude an F bonding with B and/or As, a dependence of the F incorporation on the SPE rate must be assumed.

Finally, on the regrown B-doped sample, we performed a RTA process (850 °C, 10 min) to study the F and B diffusion. We observed a considerable F outdiffusion [closed circles in Fig. 2(b)], but, in spite of this, the B profile [closed circles in Fig. 2(c)] does not suffer any diffusion at all, being identical to the implanted one. In absence of F, the expected boron TED, caused by the Is backflow from EOR defects, is instead revealed [closed squares in Fig. 2(c)]. This means that in the presence of F a clear suppression of boron TED occurs which cannot be ascribed to a B–F chemical bonding, confirming what we reported in a previous work.[6]

In conclusion, we studied the incorporation of F in Si in the presence of dopants. In Si doped with B or As a higher, local F incorporation is revealed, whereas a lower F incorporation is achieved if B and As are co-present, compensating each other. We showed that the F incorporation enhancement cannot be ascribed to a chemical bonding between F and dopants, while it is due to a kinetic effect related to the SPE rate, which is modified by the doping. These results, clarifying the F incorporation mechanism in Si, have strong implications for the application of F in the fabrication of ultrashallow junctions in future generation devices.

The authors wish to thank M. C. Camalleri, A. Messina (STMicroelectronics, Catania), and R. Storti (University of Padova) for their useful support. This work has been partially financed by the MIUR Project PRIN 2004 and FIRB.

[1]The International Technology Roadmap for Semiconductors, 2003.
[2]R. G. Wilson, J. Appl. Phys. **54**, 6879 (1983).
[3]D. F. Downey, J. W. Chow, E. Ishida, and K. S. Jones, Appl. Phys. Lett. **73**, 1263 (1998).
[4]A. Mokhberi, R. Kasnavi, P. B. Griffin, and J. D. Plummer, Appl. Phys. Lett. **80**, 3530 (2002).
[5]J. M. Jacques, L. S. Robertson, K. S. Jones, M. E. Law, M. Rendon, and J. Bennett, Appl. Phys. Lett. **82**, 3469 (2003).
[6]G. Impellizzeri, J. H. R. dos Santos, S. Mirabella, F. Priolo, E. Napolitani, and A. Carnera, Appl. Phys. Lett. **84**, 1862 (2004).
[7]R. Duffy, V. C. Venezia, A. Heringa, B. J. Pawlak, M. J. P. Hopstaken, G. C. J. Maas, Y. Tamminga, T. Dao, F. Roozeboom, and L. Pelaz, Appl. Phys. Lett. **84**, 4283 (2004).
[8]B. J. Pawlak, R. Surdeanu, B. Colombeau, A. J. Smith, N. E. B. Cowern, R. Lindsay, W. Vandervost, B. Brijs, O. Richard, and F. Cristiano, Appl. Phys. Lett. **84**, 2055 (2004).
[9]A. Claverie, B. Colombeau, B. de Mauduit, C. Bonafos, X. Hebras, G. Ben Assayag, and F. Cristiano, Appl. Phys. A: Mater. Sci. Process. **76**, 1025 (2003).
[10]P. A. Stolk, J. H.-J. Gossmann, D. J. Eaglesham, D. C. Jacobson, C. S. Rafferty, G. H. Gilmer, M. Jaraìz, J. M. Poate, H. S. Luftman, and T. E. Haynes, J. Appl. Phys. **81**, 6031 (1997).
[11]M. Y. Tsai, D. S. Day, B. G. Streetman, P. Williams, and C. A. Evans, Jr., J. Appl. Phys. **50**, 188 (1979).
[12]I. Suni, U. Shreter, M-A. Nicolet, and J. E. Baker, J. Appl. Phys. **56**, 273 (1984).
[13]G. L. Olson and J. A. Roth, Mater. Sci. Rep. **3**, 1 (1988).
[14]W. G. Pfann, *Zone Melting* (Wiley, New York, 1958).
[15]G. R. Nash, J. F. W. Schiz, C. D. Marsh, P. Ashburn, and G. R. Booker, Appl. Phys. Lett. **75**, 3671 (1999).

Downloaded 08 Jan 2007 to 192.84.150.213. Redistribution subject to AIP license or copyright, see http://apl.aip.org/apl/copyright.jsp